Electrical conduction in macroscopically oriented deoxyribonucleic and hyaluronic acid samples

Zdravko Kutnjak,* Gojmir Lahajnar, and Cene Filipič
Department of Condensed Matter Physics, Jožef Stefan Institute, P.O. Box 3000, 1001 Ljubljana, Slovenia

Rudolf Podgornik
Department of Physics, University of Ljubljana, Jadranska 19, 1000 Ljubljana, Slovenia
and Department of Theoretical Physics, Jožef Stefan Institute, P.O. Box 3000, 1001 Ljubljana, Slovenia

Lars Nordenskiöld, Nikolay Korolev, and Allan Rupprecht
Division of Physical Chemistry Arrhenius Laboratory, Stockholm University S-106 91 Stockholm, Sweden
(Received 18 June 2004; published 4 April 2005)

Measurements of the quasistatic and frequency dependent electrical conductivity below 1 MHz were carried out on wet-spun, macroscopically oriented, calf thymus deoxyribonucleic (DNA) and umbilical cord hyaluronic acid (HA) bulk samples. The frequency dependence of the electrical conductivity in the frequency range of approximately 10^{-3}–10^{6} Hz of both materials is surprisingly rather similar. Temperature dependence of the quasistatic electrical conductivity above the low temperature saturation plateau can be well described by the activated Arrhenius law with the activation energy of ≈0.8 eV for both DNA and HA. We discuss the meaning of these findings for the possible conduction mechanism in these particular charged polyelectrolytes.

DOI: 10.1103/PhysRevE.71.041901 PACS number(s): 87.14.Gg, 72.80.Le, 87.15.−v

I. INTRODUCTION

Deoxyribonucleic acid (DNA) is a polyester of phosphoric acid and 2′-deoxyribose substituted with purine or pyrimidine bases [1]. In aqueous solutions the phosphates are usually dissociated making it a highly charged polyelectrolyte. In nature DNA in general does not occur as a single chain but pairs in an antiparallel double stranded system (ds-DNA) according to the double-helical Watson-Crick base-pair model [2]. In salt solutions DNA is usually in the *B* form characterized by a 3.4-nm or 10-bp pitch, with major and minor grooves at 2.2. and 1.2 nm and an effective thickness of about 2 nm giving it a structural charge of 4.35 as measured in terms of the Manning charge parameter [1]. In aqueous solutions DNA always comes in a complex with a counterion, in our case as lithium salt, Li-DNA. It remains in the *B* form for any, except very high densities where it goes into an *A* form characterized by a thicker radius and a smaller pitch [3]. At high densities ds-DNA makes a whole slew of ordered mesophases [4] usually with a local hexagonal packing of variable spatial range except at the highest densities where it shows a monoclinic packing symmetry [5]. The existence of this zoo of ordered mesophases is due to its relatively high intrinsic stiffness on the order of 50 nm as well as its highly charged backbone [6].

Hyaluronic acid (HA) is a member of the glycosaminoglycan family and is an alternating copolymer of D-glucuronic acid and N-acetyl-D-glucosamine (for structural details see Ref. [7]) that occurs in connective tissue and mucous substances of the body [8]. In aqueous solutions its carboxyl groups are completely dissociated making HA a highly charged polyelectrolyte [9]. Just as in the case of DNA in aqueous solutions, HA always comes in a complex with a counterion, in our case as potassium salt, K-HA. The dissacharide repeat unit of HA is between 0.4 and 0.9 nm long, giving it a structural charge of about 0.72 as measured in terms of the Manning parameter [9]. Its intrinsic persistence length is on the order of 10 nm; it is thus much stiffer than a typical synthetic polyelectrolyte such as polystyrene sulfonate, but much more flexible than DNA, and multistranded polysaccharides, such as xanthan [10]. HA makes a viscoelastic solution or paste, depending on the concentration and size of the chains, even up to very high polymer concentrations. The intrinsic stiffness of HA is apparently too small to induce any mesophase formation even at the highest densities. In the crystalline state x-ray diffraction of HA at *p*H 2.0 is consistent with an extended two fold helix conformation with an axial rise per disaccharide of 0.98 nm, though this structure has never been refined. Diffraction at *p*H 3–4.5 is consistent with a left-handed four-fold helix conformation with an axial rise of 0.84 nm per disaccharide. These sinuous chains are organized as two antiparallel double helices in a tetragonal unit cell. Diffraction at *p*H 5–8 is consistent with an extended left-handed, four-fold helix of axial rise 0.95 nm per disaccharide, where two of these chains are packed in a tetragonal unit cell. Further features and details of the structure of HA in the crystalline state are provided by the different counterions [11,12]. No universality of the type seen in DNA is observed for HA at high packing density but it is generally believed that in solution HA is a single stranded helix.

Wet-spun DNA [13] as well as HA [14] at low relative humidity make macroscopically ordered samples with well characterized average molecular orientation, as shown unequivocally by Rupprecht [14]. While wet-spun DNA is always in the double stranded right-handed helical conformation, HA makes a number of distinctive arrangements with observable transitions between conformational states, de-

*URL: http://www2.ijs.si /~kutnjak

pending on the nature of the cation and the *p*H as described above [11,12]. X-ray diffraction data, taken as a whole, indicate that the conformation of HA is flexible and very sensitive to the water and cation environment with a strong preference for left-handed helical conformations.

As with all biomolecules, the molecular properties of DNA as well as HA are emergent from their respective interactions with water. These can be quantitatively inferred from the measured equation of state, i.e., the dependence of the osmotic pressure on the molecular density as measured by the osmotic stress method [15]. At high densities these interactions are dominated by hydration effects [16] which are presumably due to locally ordered water molecules on the molecular surfaces and do not depend on the presence of salt [17]. For both molecules [9,16] they can be codified in terms of a hydration force decaying spatially with a characteristic length of between 0.2 and 0.3 nm. No such similarity exists in the regions dominated by the salt effects where DNA shows a clear imprint of molecular conformational fluctuations while HA has a much less universal behavior [9].

The conductance properties of DNA have recently attracted substantial interest from both the theoretical as well as the experimental sides [18–21]. Understanding the charge transfer mechanism along DNA double helix is important in long-range chemistry of oxidative DNA damage and repair processes, monitoring protein-DNA interactions, and for possible applications in nanoelectronic circuit technology [19,22,23]. However, despite intensive investigations the nature of the charge transfer mechanism remains a subject of controversy. Various measurements suggest both short and long-range charge migration [18,19,24,25] with some indication that the ds-DNA can behave like a one dimensional molecular wire [26].

We recently extended these studies of molecular conductivity to the case of macroscopically oriented wet-spun bulk samples of DNA at low humidity [27], where, contrary to most single-molecule studies, one can control the orientation of the molecules as well as unequivocally ascertain their molecular integrity. The price one has to pay for this certainty is that the conductivity measurements are performed on a macroscopic sample.

Since most of the results on DNA conduction properties, single molecule as well as macroscopically oriented bulk samples, have been interpreted in terms of mechanisms specific for its molecular structure and conformation, it should be of some interest to investigate also the possible similarities in polyelectrolyte charge conduction by extending the measurements to the realm of other polyelectrolytes. Having in mind experiments on oriented macroscopic samples, HA seems to be a likely candidate. It is sufficiently similar to DNA in the sense that it can make macroscopically oriented wet-spun samples of the same type as DNA, but is molecularly and conformationally far removed from it, so it is not unreasonable to expect that any specific mechanisms of conduction in both polyelectrolytes, if indeed they do exist, should be quite different from one another.

In this contribution we present quasistatic measurements of the temperature dependent electrical conductivity obtained on both native wet-spun calf thymus Li-DNA [27] and native wet-spun umbilical cord K-HA in a dc measuring field and measurements of the frequency dependent conductivity at low frequencies between 20 Hz and 1 MHz. We show that the electrical conductivity in the frequency range of $\approx 10^{-3}$–10^{6} Hz for both systems is comparable, thus indicating that some aspects of the conducting mechanism could be shared by both systems. A fact that both systems are covered by vicinal water layers points to a conducting mechanism most likely mediated by their respective interactions with hydrating water molecules.

II. EXPERIMENTAL PROCEDURES

Wet-spun oriented samples were prepared from calf thymus Li-DNA (Pharmacia) with a molecular weight of 10^7, corresponding to a contour length of about 5 μm or some 10^2 persistence lengths of 50 nm, by wet spinning and then drying [28]. The wet spinning method allows for controlled production of sufficient amounts of highly macroscopically oriented thin films by spooling DNA fibers that are continuously stretched during precipitation into an aqueous alcohol solution. The dried Li-DNA sheets of thickness of about 3–4 mm and surface area between 10 and 20 mm^2 were then cut perpendicularly to the orientational axis of the DNA molecules into bulk samples of $6.4 \times 4.4 \times 3.4$ mm^3 that were used in conductivity measurements.

Wet-spun oriented samples of K-HA have been prepared by exactly the same method as in the case of DNA [28] from high molecular weight potassium hyaluronate isolated from human umbilical cord, corresponding to a contour length of about 10 μm or some 10^3 persistence lengths of 10 nm. The dried wet-spun K-HA at 75% relative humidity shows a diffraction pattern consistent with fourfold helical arrangement as observed in other studies [14]. The samples used in the conductivity experiments displayed a high degree of molecular orientation with good crystallinity and consisted of concertinalike parallelepipedic forms of dimensions $5.5 \times 4 \times 3$ mm^3 containing many layers of wet-spun K-HA films.

Quasistatic resistivity and *I-V* curve measurements were performed by a Keithley 617 programmable electrometer on samples kept in either 60% or 75% relative humidity (r.h.) and on samples dried in vacuum. The quasistatic measurements were performed for several values of the excitation dc electric field between 1 and 300 V/cm. The time scale of the quasistatic experiment determined by both the data sampling time and the temperature cooling rate was estimated to be of the order of 10^{-3} Hz. The offset thermocouple current due to the unavoidable temperature gradient in the lead wiring, limits the lowest value of the electrical conductivity. This thermal offset current, which is present in the same polarity was revealed in a separate measurement by so called "offset compensation technique" in which the polarity of the measuring voltage is reversed every other reading.

Frequency dependent conductivity was measured between 20 Hz and 1 MHz via measurements of the imaginary part of the complex dielectric constant by using a HP4284A Precision LCR meter. The amplitude of the excitation ac electric field was kept <60 V/cm. Gold electrodes were pressed on both sides of the sample. No difference was observed if gold

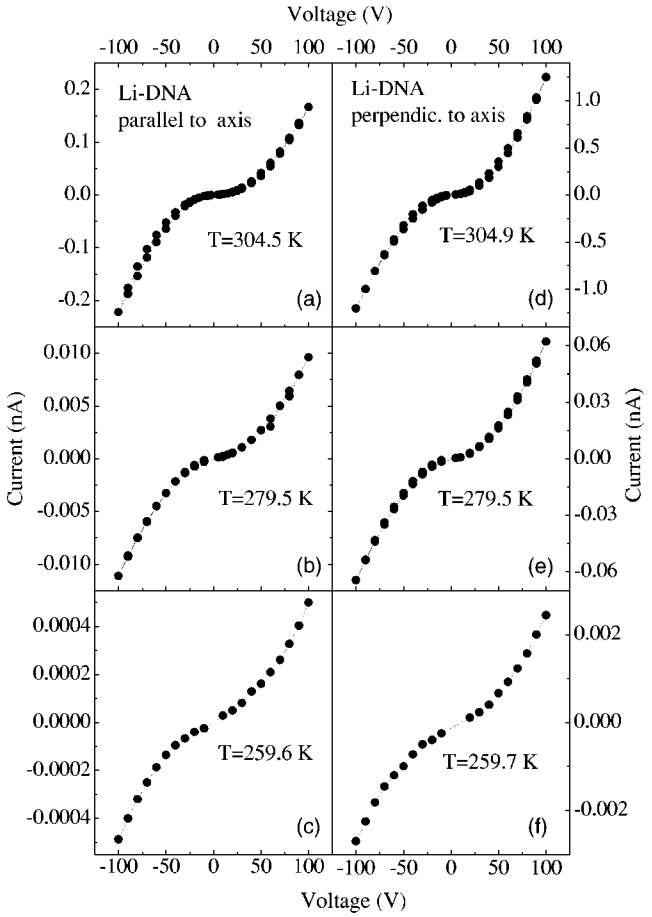

FIG. 1. Current-voltage curves measured at 75% relative humidity at various temperatures on Li-DNA. (a)–(c) The dc electric field was applied parallel to the duplex axis. (d)–(f) The dc electric field was applied perpendicular to the duplex axis.

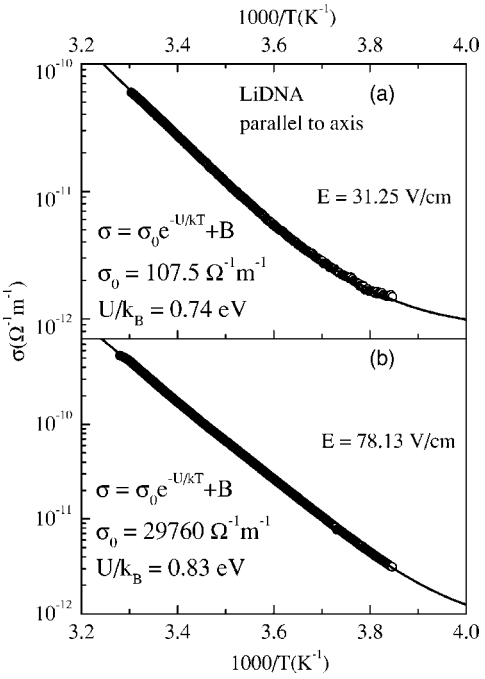

FIG. 2. Temperature dependence of the electrical conductivity measured at 75% relative humidity on Li-DNA. The DC electric field 31.25 V/cm (a) and 78.13 V/cm (b) was applied parallel to the sample orientational axis.

electrodes were replaced by some other metallic electrodes like, for instance, copper electrodes. Results were checked on various other sample geometries including 20–120-μm-thick films with typical lateral dimensions of 4 $\times 5$ mm^2. The electrical conductivity was measured either parallel to the long orientational axis or perpendicular to it, for both DNA and HA samples. In temperature scanning runs the electrical conductivity was measured on cooling the sample with the typical cooling rate of 30 K/h.

III. EXPERIMENTAL RESULTS

A. DNA results

Electrical current as a function of voltage (*I-V* curves) for wet-spun Li-DNA samples measured parallel and perpendicular to the DNA orientational axis are shown for three different temperatures in Figs. 1(a)–1(f). A weak anisotropy of $I_\perp / I_\parallel \approx 3$ was found in reasonable agreement with previously published [27] $\sigma_\perp / \sigma_\parallel \approx 3$ for higher voltages. Here current was recalculated to same sample length in order to account for different geometries in two experiments. Absence of the visible plateau in the *I-V* curve at room temperature for Li-DNA bulk samples indicates that the gap voltage is smaller than the value which can be resolved at room temperature. This result is otherwise consistent with findings on (Zn) λ-DNA [29]. Moreover, taking account of the size of the samples, it was found that the field dependent conductivity $\sigma_\parallel(E)$ of Li-DNA obtained from data in Fig. 1(a) agrees quantitatively with estimates of $\sigma(E)$ obtained from (Zn) λ-DNA data in Ref. [29]. Due to the rapid increase of the resistivity with decreasing temperature, the electric current at given voltage decreases for about one order of magnitude per decrease in temperature of about 20 K for both axis orientations [see Figs. 1(a)–1(f)]. Also nearly linear region around 0 V becomes steeper with decreasing temperature.

The influence of the electric field on the temperature dependence of both $\sigma_\parallel(T,E)$ and $\sigma_\perp(T,E)$ was verified by measuring the resistivity upon cooling the sample at several different values of the dc voltage. The quasistatic resistivity of Li-DNA samples could be followed reliably down to about 220 K, since on further cooling it begins to exceed the electrometer limiting value of $\approx 10^{16}$ Ω. Figures 2 and 3 show temperature dependence of $\sigma_\parallel(T,E)$ and $\sigma_\perp(T,E)$, respectively, taken at two different values of the electric field. Similar to measurements of *I-V* curves a weak anisotropy of $\sigma_\perp / \sigma_\parallel \approx 4$ was found around room temperature also at lower voltage values.

Similar to observations at microwave and optical frequencies [30,31], both $\sigma_\parallel(T)$ and $\sigma_\perp(T,E)$ decrease strongly below room temperature with a crossover to a saturated constant value at temperatures below 230 K. It turned out that the crossover observed in our quasistatic measurements was partly modulated by a previously mentioned thermocouple voltage offset in resistance measurements due to the unavoidable temperature gradient in the lead wiring. This offset

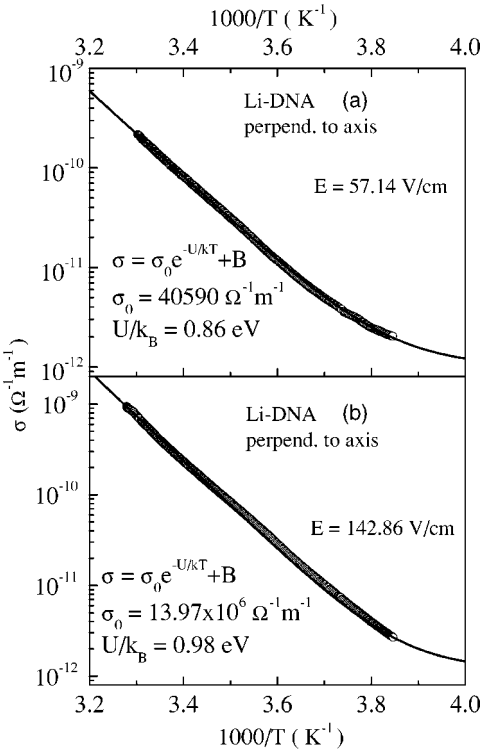

FIG. 3. Temperature dependence of the electrical conductivity measured at 75% relative humidity on Li-DNA. The dc electric field 57.14 V/cm (a) and 142.86 V/cm (b) was applied perpendicular to the sample orientational axis.

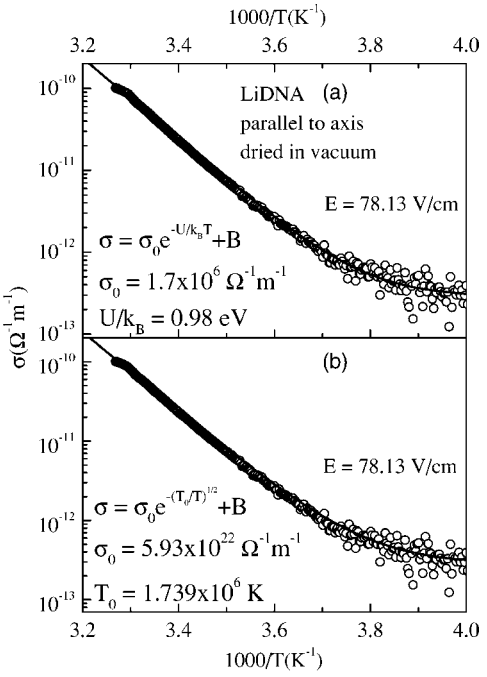

FIG. 4. Temperature dependence of the electrical conductivity measured on dried Li-DNA. Shown are fits to an Arrhenius ansatz (a) and to the ansatz describing the variable range hopping (b). Here the electric field was applied parallel to the sample orientational axis.

thermocouple current reflects itself in temperature dependence of σ as an additive nearly constant background. However, additional analysis and data obtained at higher frequencies (shown later) suggest that below $\approx$220 K indeed a crossover to nearly temperature independent σ takes place (constant B in Figs. 2 and 3).

Taking this experimental effect into account it was found that the temperature dependence of the quasistatic conductivity could be well described by a thermally activated Arrhenius ansatz,

$$\sigma = \sigma_0 e^{-(U/kT)}, \tag{1}$$

down to about 220 K temperature [see Figs. 2(a), 2(b), 3(a), and 3(b) for relevant fit parameters).

Data presented in Figs. 1–3 reveal that the electric-field dependence of σ is mainly hidden in the field dependence of the prefactor σ_0 in Eq. (1). Namely, by increasing the electric field by a factor of ≈ 3, σ_0 increases by more that two orders of magnitude, while the activation energy U remains practically the same within the experimental error of ± 0.05 eV. It thus seems that the nonlinear I-V curves are mainly a consequence of the electric-field induced increase of the charge carrier number.

In order to study the influence of the water content on the electrical conductivity Li-DNA samples were dried in vacuum for more than 24 h at room temperature. Figure 4 shows measurements of $\sigma_{\parallel}(T,E)$ performed on dried Li-DNA sample. Significant decrease in conductivity for almost one order of magnitude was observed. It should be noted that this decrease is in qualitative agreement with recent calculations [32]. Detailed analysis shows that changes in both σ_0 and U are significant. It was found that σ_0 actually increases by slightly less than two orders of magnitude and U by about 0.1 eV. The former effect is thus the dominant in decreasing the conductivity. This supports the idea [31] that rather than lower carrier number, stronger localization effects due to less regular B form of DNA may be responsible for lower DNA conductivity in water-poor environment.

It should be noted that the temperature dependence of σ presented in Figs. 2–4 including the $\sigma_{\perp}(T,E)$ data could also be fitted to the variable range hopping ansatz,

$$\sigma = \sigma_0 e^{-(T_0/T)^{\beta}}, \tag{2}$$

with 95% Fischer-Snedecor (F) test confidence level [see Figs. 4(b) and 5]. Although the systematically larger χ^2 values were found for data above 230 K, the variable range hopping ansatz becomes more successful in describing the conductivity data in a crossover region near 220 K and below.

There is an obvious discrepancy in the temperature dependence of σ between the quasistatic data and data obtained at very high frequencies [30,31]. Namely, in the case of microwave and optical measurements [30,31] the above crossover to nearly temperature independent σ occurs already at higher temperatures around 250 K. In order to check the influence of the experimental time scale on the temperature dependence of σ, i.e., on the crossover temperature region we performed additional measurements of $\sigma_{\parallel}(T)$ at various frequen-

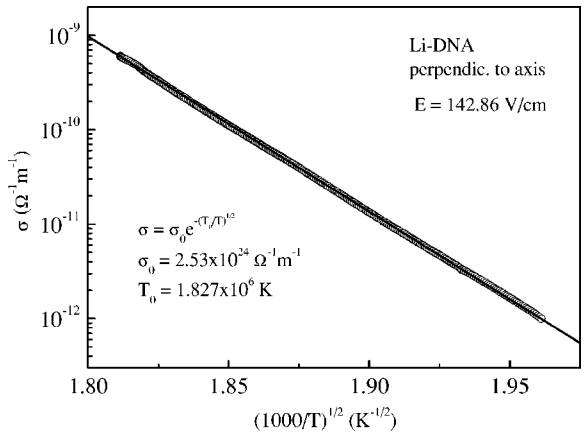

FIG. 5. Temperature dependence of the electrical conductivity measured on Li-DNA with the electric field applied perpendicular to the sample orientational axis. Shown is the fit to the ansatz describing the variable range hopping.

cies. Figure 6 shows the temperature dependence of the electrical conductivity measured parallel to the Li-DNA long orientational axis at frequencies between 20 Hz and 1 MHz.

Data presented in Fig. 6 represent effective conductivity $\sigma(\omega)=\varepsilon''\varepsilon_0\omega$ deduced from measurements of the imaginary part ε'' of the complex dielectric constant $\varepsilon^*=\varepsilon'-i\varepsilon''$. In the case of ac conductivity measurements there is no problem with the thermocouple voltage offset, as in the case of dc-type measurements. Namely, polarity of the measuring voltage is reversed every sine period. Below room temperature, the electrical conductivities at different frequencies decrease strongly with decreasing temperature, exhibiting a crossover to saturated almost constant values at lower temperatures. It is shown that actual crossover temperature depends on the frequency. Namely, data taken at higher frequencies exhibit the crossover at higher temperatures (see Fig. 6). This explains the huge difference between the crossover onset obtained at GHz frequencies and in our quasistatic mHz data. According to the theoretical calculations, at lower temperatures a crossover occurs to a mechanism with rather small activation energy or a multichannel tunneling [33].

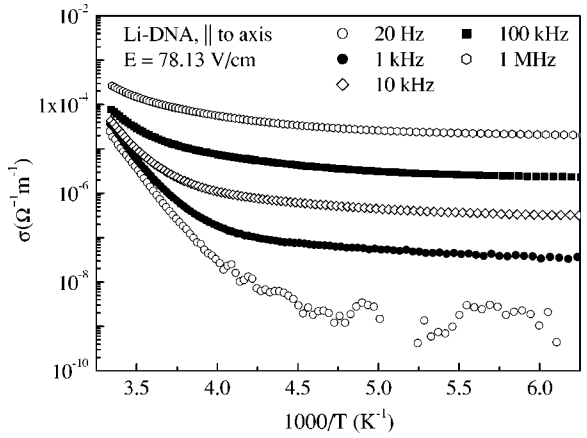

FIG. 6. Temperature dependence of the electrical conductivity measured parallel to the long Li-DNA orientational axis at several frequencies between 20 Hz and 1 MHz. The amplitude of the measuring ac electric field was 78.13 V/cm.

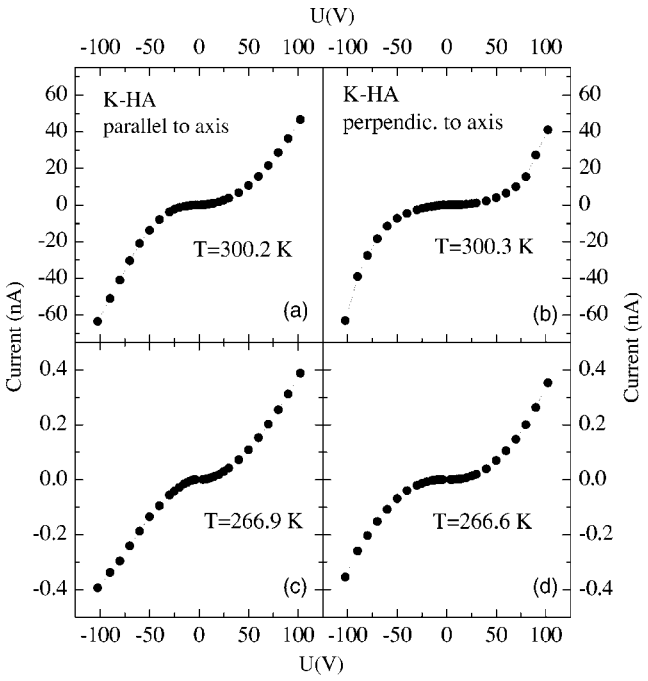

FIG. 7. Current-voltage curves measured at 60% relative humidity at two temperatures on hyaluronic acid. (a), (b) the dc electric field was applied parallel to the long orientational axis. (c), (d) the dc electric field was applied perpendicular to the long orientational axis.

B. HA results

I-V curves for wet-spun K-HA samples measured parallel and perpendicular to the HA orientational axis are shown for two different temperatures in Figs. 7(a)–7(d). In contrast to Li-DNA results, no anisotropy of $I_\perp/I_\parallel \approx 1$ was detected (compare Figs. 7(a) and 7(b) to Figs. 7(c) and 7(d)). This isotropy of conductivity could be related to a higher flexibility of HA molecules, that exhibit a persistence length of $\sim$10 nm [10], as opposed to DNA's $\sim$50 nm [1], and eventually to the fact that DNA makes a slew of ordered mesophases at higher densities while HA does not. The macroscopically oriented wet-spun K-HA sample could thus be much more disordered on the relevant microscopic length scales than Li-DNA leading to a more thorough microscopic washing out of the macroscopic anisotropies.

Absence of the visible plateau in the *I-V* curves for wet-spun K-HA bulk samples indicates that (like in DNA samples) the gap voltage is smaller than the value which can be resolved at room temperature. Furthermore, just as in the case of Li-DNA, K-HA samples show a rapid increase of resistivity with decreasing temperature. The electric current at given voltage decreases for about two orders of magnitude per decrease in temperature of about 35 K for both axis orientations [see Figs. 7(a)–7(d)].

The temperature dependence of $\sigma_\parallel(T,E)$ was obtained by measuring the resistivity upon cooling the sample at two different values of the dc voltage as well as on in-vacuum

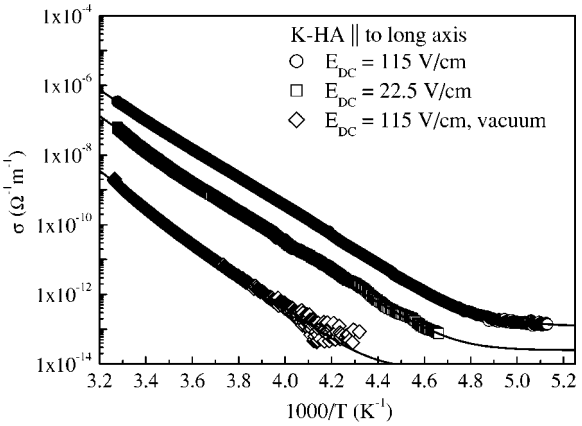

FIG. 8. Temperature dependence of the electrical conductivity measured at 60% relative humidity and on dried hyaluronic acid. The dc electric field was applied parallel to the sample orientational axis. Solid lines represent fits to the ansatz describing the variable range hopping.

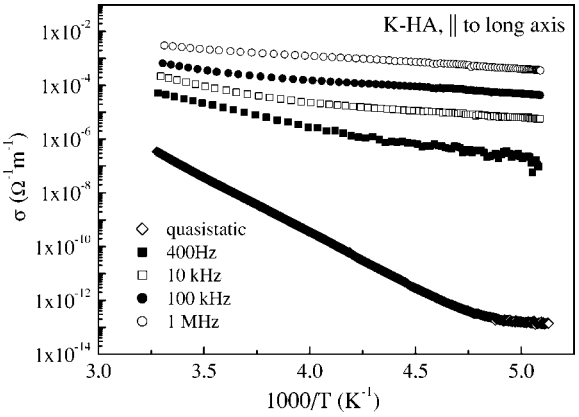

FIG. 9. Temperature dependence of the electrical conductivity measured parallel to the long K-HA orientational axis at several frequencies between 400 Hz and 1 MHz. The amplitude of the measuring ac electric field was 115 V/cm. The quasistatic data are also shown for comparison.

dried sample. Figure 8 shows the temperature dependence of $\sigma_{\parallel}(T,E)$, taken at the electric fields of 22.5 and 115 V/cm. The time scale of the quasistatic experiment was slightly shorter than in the case of Li-DNA measurements, i.e., it was estimated to be of the order of 6×10^{-3} Hz. Similar to Li-DNA, $\sigma_{\parallel}(T)$ of K-HA decreases strongly below room temperature with a crossover to a saturated constant value at temperatures around 200 K, i.e., at slightly lower temperatures than in the case of the Li-DNA.

The temperature dependence of the conductivity could be well described by a thermally activated Arrhenius ansatz (1) for temperatures above the crossover region with very similar fit parameters as in the case of Li-DNA: $U/k_B=0.83$ eV, $\sigma_0=7.6\times10^6\ \Omega^{-1}\,\mathrm{m}^{-1}$, and $4.9\times10^7\ \Omega^{-1}\,\mathrm{m}^{-1}$ for $E=22.5$ and $E=115$ V/cm, respectively. This demonstrates that the electric-field dependence of σ in K-HA is also related to the electric-field induced increase of the charge carrier number.

Figure 8 also shows measurements of $\sigma(T,E)$ performed on K-HA dried in vacuum for about 24 h at room temperature. In contrast to Li-DNA, slightly larger decrease in conductivity for almost two orders of magnitude was observed. Here, both $\sigma_0=1.5\times10^7\ \Omega^{-1}\,\mathrm{m}^{-1}$ and $U/k_B=0.95$ eV contribute to decreasing the conductivity in contrast to Li-DNA.

It should be noted that the temperature dependence of σ presented in Fig. 8 could be very well fitted in a broad temperature range to the variable range hopping ansatz (2) (see solid lines in Fig. 8), with similar fit parameters as obtained for Li-DNA: $T_0=1.6\times10^6$ K, $\sigma_0=1.6\times10^{24}\ \Omega^{-1}\,\mathrm{m}^{-1}$, and $T_0=1.4\times10^6$ K, $\sigma_0=3.0\times10^{22}\ \Omega^{-1}\,\mathrm{m}^{-1}$ for $E=22.5$ V/cm and $E=115$ V/cm, respectively, and $T_0=1.9\times10^6$ K, $\sigma_0=9.9\times10^{24}\ \Omega^{-1}\,\mathrm{m}^{-1}$ for the dried sample. This demonstrates that although slightly different temperature dependence was obtained in K-HA samples, the underlying conductivity mechanism must be similar.

Figure 9 shows temperature dependence of the $\sigma_{\parallel}(T,\omega)$ measured parallel to the K-HA long orientational axis at frequencies between 400 Hz and 1 MHz. Frequency dependent conductivity presented in Fig. 9 was obtained in same way as Li-DNA data via measurements of the imaginary part $\sigma(\omega)=\varepsilon''\varepsilon_0\omega$ of the complex dielectric constant. In the case of K-HA the electrical conductivities at different frequencies exhibit slightly different temperature dependence than the Li-DNA frequency dependent data (compare Figs. 6 and 9). $\sigma_{\parallel}(\omega)$ curves decrease rather less strongly below room temperature than in the case of Li-DNA data, with a crossover to another activatedlike regime at lower temperatures with smaller activation energy (slopes in Fig. 9), rather than in a temperature independent regime as in the case of Li-DNA. However, data taken at higher frequencies exhibit a crossover at higher temperatures (see Fig. 9), i.e., the actual crossover temperature depends in a similar way on the frequency as in the Li-DNA case. Although no saturated regime could be observed in $\sigma_{\parallel}(T,\omega)$ for temperatures down to 150 K for high frequency data, the existence of the saturated plateau in quasistatic data suggests that there must be a crossover at lower frequencies to a qualitatively different temperature dependence more similar to that observed in Li-DNA.

IV. DISCUSSION

Our conductance measurements for macroscopically ordered samples of two biologically important polyelectrolytes, DNA and HA, point to definite similarities as well as differences in both the frequency and temperature behavior of conductivity.

The similarities between the two systems, clearly discernible from the frequency dependence of the conductivity, see Fig. 10, could probably originate from the similar underlying conductivity mechanisms. DNA and HA are structurally unrelated, but in aqueous environments they do share the same structured water vicinal layers, as conclusively demonstrated by the measurements of the equation of state [9,16]. Thus the similarities in their frequency dependent conductivity might point to a common or related charge carrier hopping mechanism that could originate in the interactions between the structural backbone of the molecules and the highly struc-

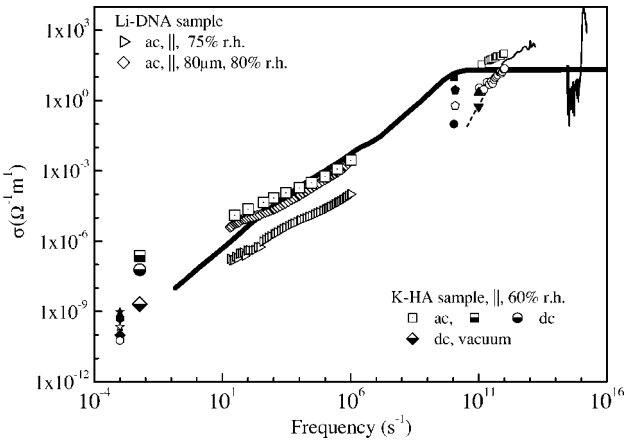

FIG. 10. Frequency dependence of the conductivity obtained with λ-DNA, calf thymus wet-spun oriented Li-DNA, and wet-spun oriented K-HA. The thick solid line denotes model calculations [21]. Other high frequency data above 1 MHz are taken from Refs. [30,31,37]. Data obtained on an 80-μm-thick calf thymus Li-DNA film are denoted by $\diamondsuit$. Orientation of the applied electric field relative to the macroscopic orientational axis of the sample is denoted by $\parallel$ and $\perp$. Note that data at 10^{-3} Hz and $\approx 10^{-2}$ Hz correspond to quasistatic conductivity of DNA and HA molecules, respectively. Most of the data scattering could be attributed to different relative humidity environments. See also Ref. [27] for more details.

tured vicinal water layers on the surface of both macromolecules.

It was shown recently that coupling of the conductive chain to an external environment could induce different electronic states in the DNA conductance spectrum, where the external environment could be described either as a general dissipative medium [34] or more specifically as a water environment [32].

It should be stressed that the conductivity measurements extended down to the quasistatic experimental time scale and earlier high frequency DNA data up to 10^{15} Hz agree qualitatively with theoretical results (solid line in Fig. 10) based on the hopping hole conduction mechanism [21]. Some caution should nevertheless be exercised when comparing our data on macroscopic samples with existing calculations on single chains since the calculations do not yet take into account the structured water environment in the vicinal layers, which we hypothesize might be important to understand the observed similarity in the conductivity behavior of DNA and HA.

Although our quasistatic electrical conductivity data point to only two mechanisms (hopping at high temperatures and possible tunneling at low temperatures), which contribute to the dc conductivity, we do not actually exclude the possibility that also other mechanisms might contribute to the conductivity at very high frequencies in the GHz range (see indications for that in Refs. [27,35,36]). On the other hand, the differences in behavior of the K-HA conductivity such as lack of anisotropy, two orders of magnitude larger dc conductivity value at room temperature, larger decrease of conductivity in dry environment, shift of saturated plateau region to lower temperatures, and different temperature dependence of conductivity at higher frequencies in comparison to Li-DNA conductivity are most probably related to dissimilar molecular structure and higher flexibility of HA molecules. It is the structural parameters of both macromolecules, such as the wide gap in their persistence lengths, that leads to a more pronounced molecular disorder as inferred from the absence of any anisotropy in the *I-V* response in the case of a more flexible HA, persistence length 10 nm, when compared to stiffer DNA, persistence length 50 nm. This absence of *I-V* anisotropy could thus be directly related to the absence of any mesophases between the isotropic solution and a crystal in the case of HA and in distinction from DNA.

Our measurements are most definitely not single molecule experiments. We measure properties of bulk but, nevertheless, highly oriented phases. This has its own advantages as well as pitfalls. While we have complete control over the orientation of the macromolecules, the nature of their counterions and can unequivocally ascertain their molecular integrity, we have basically no handle on the DNA secondary structure such as bends and nicks. These conditions can be much better handled in single molecule experiments [38,39]. On the other hand these same single molecule experiments are invariably connected with radical DNA treatment such as complete drying that can be very detrimental to molecular integrity.

Furthermore, the path from bulk sample experiments to single molecule conductivity is admittedly not straightforward and one cannot naively assume that the bulk sample conductivity is the sum of single molecule conductivities. In bulk samples there is no continuity of the molecules from one electrode to the other one since they are too short to span the entire macroscopic sample. However, for DNA samples one can argue that the gaps between molecules do not radically alter their molecular continuity due to exposed hydrophobic cores at their ends that tend to associate very closely. This is the primary reason why monodisperse DNA fragments do not make a smectic phase just before entering the crystalline phase as beautifully argued by Livolant *et al.* [40]. Unfortunately no such argument exists for the case of HA and molecular continuity or the lack thereof can have stronger repercussions in this system.

V. CONCLUSIONS

We measured conductivities of bulk oriented wet-spun samples of Li-DNA and K-HA. Several features of the electrical conductivity of both molecular systems are comparable. For instance, the dc conductivity of both molecular systems at room temperature being within $\sim 10^{-8}$–10^{-10} Ω^{-1} m^{-1}. *I-V* measurements in macroscopically oriented wet-spun bulk samples of K-HA and Li-DNA show that the nonlinearity of the *I-V* curves could be attributed in both systems to the electric-field induced increase of the charge carrier number. The frequency dependence of the electrical conductivity in the frequency range of approximately 10^{-3}–10^{6} Hz of both materials is surprisingly similar. Temperature dependence of the quasistatic electrical conductivity above the saturated plateau temperature region can be

well described by the activated Arrhenius law with the activation energy of ≈ 0.8 eV for both the DNA and HA.

The observed similarities in the frequency dependent conductivity indicate a common charge carrier hopping mechanism originating probably in the interactions between the structural backbone of the molecules with the highly structured vicinal water layers on the surface of both macromolecules. The effects of these vicinal water layers have only begun to be considered by theorists [32,34] and at present the (single chain) calculations are not yet at the stage where direct comparison with our experiments would make sense. A realistic theoretical model would have to include many chains coupled via external environment.

The differences in behavior of the conductivity between two systems such as different anisotropy, different decrease of conductivity in dry environment, and saturation of the conductivity at different temperatures could, on the other hand, are most probably related to different molecular structure and to much higher flexibility of HA molecules.

ACKNOWLEDGMENTS

This research was supported by the Slovenian Office of Science under Program Nos. P1-0125 and P1-0055 and Project No. J1-6593-0106-04.

[1] V. A. Bloomfield, D. M. Crothers, and I. Tinoco, *Nucleic Acids* (University Science Books, New York, 2000).
[2] R. R. Sinden, *DNA Structure and Function* (Academic Press, New York, 1994).
[3] S. M. Lindsay, S. A. Lee, J. W. Powell, T. Weidlich, C. Demarco, G. D. Lewen, N. J. Tao, and A. Rupprecht, Biopolymers **27**, 1015 (1988).
[4] H. H. Strey, R. Podgornik, D. Rau, and V. A. Parsegian, Curr. Opin. Struct. Biol. **8**, 309 (1998).
[5] F. Livolant and A. Leforestier, Prog. Polym. Sci. **21**, 1115 (1996).
[6] R. Podgornik, H. H. Strey, and V. A. Parsegian, Curr. Opin. Colloid Interface Sci. **3**, 534 (1998).
[7] D. Voet and J. G. Voet, *Biochemistry* (Wiley and Sons, New York, 1990).
[8] H. G. Elias, *Macromolecules* (Plenum Press, New York, 1984).
[9] R. M. Peitzsch and W. F. Reed, Biopolymers **32**, 219 (1992).
[10] S. Ghosh, X. Li, C. E. Reed, and W. F. Reed, Biopolymers **30**, 1101 (1998).
[11] J. K. Sheehan and E. D. T. Atkins, Int. J. Biol. Macromol. **5**, 215 (1983).
[12] J. K. Sheehan, K. H. Gardner, and E. D. T. Atkins, J. Mol. Biol. **117**, 113 (1977).
[13] A. Rupprecht, Biopolymers **9**, 825 (1970).
[14] A. Rupprecht, Acta Chem. Scand., Ser. B **B33**, 779 (1979).
[15] V. A. Parsegian, R. P. Rand, and D. C. Rau, Methods Enzymol. **259**, 43 (1995).
[16] R. Podgornik, D. C. Rau, and V. A. Parsegian, Macromolecules **22**, 1780 (1989).
[17] S. Leikin, V. A. Parsegian, D. C. Rau, and R. P. Rand, Annu. Rev. Phys. Chem. **44**, 369 (1993).
[18] F. D. Lewis, T. F. Wu, Y. F. Zhang, R. L. Letsinger, S. R. Greenfield, and M. R. Wasielewski, Science **277**, 673 (1997).
[19] E. M. Boon and J. K. Barton, Curr. Opin. Struct. Biol. **12**, 320 (2002).
[20] R. Bruinsma, G. Gruner, M. R. D'Orsogna, and J. Rudnick, Phys. Rev. Lett. **85**, 4393 (2000).
[21] Y.-J. Ye, R.-S. Chen, A. Martinez, P. Otto, and J. Ladik, Solid State Commun. **112**, 139 (1999).
[22] M. R. Arkin, E. D. A. Stemp, R. E. Holmlin, J. K. Barton, A. Hormann, E. J. C. Olson, and P. F. Barbara, Science **273**, 475 (1996).
[23] M. D. Purugganan, C. V. Kumar, and J. K. Barton, Science **241**, 1645 (1988).
[24] D. B. Hall, R. E. Holmlin, and J. K. Barton, Nature (London) **382**, 731 (1996).
[25] P. T. Henderson, D. Jones, G. Hampikian, Y. Kan, and G. B. Schuster, Proc. Natl. Acad. Sci. U.S.A. **96**, 8353 (1999).
[26] J. M. Warman, M. P. de Haas, and A. Rupprecht, Chem. Phys. Lett. **249**, 319 (1996).
[27] Z. Kutnjak, C. Filipič, R. Podgornik, L. Nordenskiöld, and N. Korolev, Phys. Rev. Lett. **90**, 098101 (2003).
[28] A. Rupprecht, Acta Chem. Scand. **2**, 477 (1966).
[29] A. Rakitin, P. Aich, C. Papadopoulos, Y. Kobzar, A. S. Vedeneev, J. S. Lee, and J. M. Xu, Phys. Rev. Lett. **86**, 3670 (2001).
[30] P. Tran, B. Alavi, and G. Gruner, Phys. Rev. Lett. **85**, 1564 (2000).
[31] E. Helgren, A. Omerzu, G. Gruner, D. Mihailovic, R. Podgornik, and H. Grimm, cond-mat/0111299.
[32] Y.-J. Ye, R. S. Chen, F. Chen, J. Sun, and J. Ladik, Solid State Commun. **119**, 175 (2001).
[33] L. Shen, Y.-J. Ye, and J. Ladik, Solid State Commun. **121**, 35 (2002).
[34] R. Gutiérrez, S. Mandal, and G. Cuniberti, cond-mat/0410660.
[35] N. P. Armitage, M. Briman, and G. Gruner, Phys. Status Solidi B **241**, 69 (2004).
[36] M. Briman, N. P. Armitage, E. Helgren, and G. Gruner, Nano Lett. **4**, 733 (2004).
[37] A. Wittlin, L. Genzel, F. Kremer, S. Haseler, A. Poglitsch, and A. Rupprecht, Phys. Rev. A **34**, 493 (1986).
[38] B. Hartzell, B. McCord, D. Asare, H. Chen, J. J. Heremans, and V. Soghomonian, Appl. Phys. Lett. **82**, 4800 (2003).
[39] B. Hartzell, B. McCord, D. Asare, H. Chen, J. J. Heremans, and V. Soghomonian, J. Appl. Phys. **94**, 2764 (2003).
[40] F. Livolant, A. M. Levelut, J. Doucet, and J. P. Benoit, Nature (London) **339**, 724 (1989).